FACTA UNIVERSITATIS
Series: **Physics, Chemistry and Technology** Vol. 18, Nº 2, 2020, pp. 131 - 139
https://doi.org/10.2298/FUPCT2002131D

SINGLE-ELECTRON CAPTURE IN ION-ION COLLISIONS†

UDC 539.186

Danilo Delibašić, Nenad Milojević, Ivan Mančev

University of Niš, Department of Physics, Faculty of Sciences and Mathematics, Niš, Serbia

Abstract. *The prior versions of the three-body boundary-corrected first Born approximation (CB1-3B) and the three-body boundary-corrected continuum intermediate states method (BCIS-3B) are applied to calculate the state-selective and state-summed total cross sections for single-electron capture from hydrogen-like ion targets* (He^+, Li^{2+}) *by fast completely stripped projectiles* (H^+, He^{2+}, Li^{3+}). *All calculations are carried out for single-electron capture into arbitrary nlm final states of the projectiles, up to* $n = 4$. *The contributions from higher n shells are included using the Oppenheimer* n^{-3} *scaling law. The present results are found to be in satisfactory agreement with the available experimental data.*

Key words: *ion-ion collisions, electron capture*

1. INTRODUCTION

The phenomenon of electron capture in fast ion-atom collisions has been a focus of scientific research for almost a full century, with the first steps dating back to the pioneering work of Oppenheimer, 1928 and Brinkman and Kramers, 1930. Numerical values of cross sections for such a process provide us with a fundamental insight, while also carrying substantial practical interest. Since electron capture cross sections are essential in estimating the energy losses of ions during their passage through varying kinds of matter, their databases have very useful applications in a wide array of areas. These range from predominately theoretical, such as plasma physics, astrophysics, and heavy-ion transport physics, to more practically-oriented, such as fusion energy research, as well as medical physics (hadron therapy in cancer patients).

Received August 4th, 2020; accepted October 28th, 2020
†Acknowledgement: The authors thank the support by the Ministry of Education, Science and Technological Development of the Republic of Serbia under Contract No. 451-03-68/2020-14/200124.
Corresponding author: Danilo Delibašić, Department of Physics, Faculty of Sciences and Mathematics, University of Niš, Višegradska 33, 18000 Niš, Serbia
E-mail: danilo.delibasic@pmf.edu.rs

In the present work, we investigate the processes of single-electron capture in collisions between fast completely stripped projectiles and hydrogen-like ions in their ground state, by calculating their corresponding state-selective and state-summed total cross sections. These are genuinely three-body processes which, as such, represent critical tests to the validity of three-body theories. The presented cross sections are calculated in the frameworks of the prior versions of the three-body boundary-corrected first Born approximation (CB1-3B) and the three-body boundary-corrected intermediate states method (BCIS-3B). The CB1-3B method represents the first-order term in the perturbation expansion of the exact eikonal transition amplitude. The prior form of the BCIS-3B method uses the same perturbation potential and asymptotic wavefunction in the entrance channel as the prior form of the CB1-3B method, whereas the asymptotic wavefunction in the exit channel is distorted by the full continuum wave associated with the electron-target interaction. In this sense, BCIS-3B is a second-order theory. Since CB1-3B and BCIS-3B methods employ the eikonal hypothesis, they are both high energy theories and are therefore expected to produce very good results primarily in the high energy region, with possibly limited success in the intermediate energy region.

The CB1-3B method, first developed in the work of Belkić et al., 1979, was successfully applied to single-electron capture (Belkić et al., 1986, Belkić and Taylor, 1987, Belkić et al., 1987b), and subsequently extended to a four-body theory, in the framework of the four-body boundary-corrected first Born approximation (CB1-4B) by Mančev et al., 2012. The CB1 methods have a long history of application to the ground-to-arbitrary state capture process. The boundary-corrected continuum intermediate states method was first introduced for double-electron capture within a four-body formalism (BCIS-4B) by Belkić (Belkić, 1993), and subsequently adapted and applied to single-electron capture within both four-body (Mančev et al., 2015) and three-body formalisms (Mančev et al., 2018). All these applications of BCIS methods were performed for ground-to-ground state capture, with the first generalization to ground-to-arbitrary state capture being done recently by Milojević et al. (2020). All these works showed a systematic agreement with available measurements at intermediate and high energy values, for both CB1 and BCIS methods. Note that both these approximations are fully quantum-mechanical approaches, with the correct boundary conditions being strictly preserved, in both the entrance and exit collision channels. Whenever the ion-atom collision aggregates are charged in the asymptotic channels, correct boundary conditions should be fully considered in both collision channels (Belkić, 2004, Belkić, 2008). Some of the processes with single-electron capture considered in this paper were previously analyzed in the frameworks of various approaches (Mukherjee and Sil, 1980, Samanta et al., 2010, Grozdanov and Solov'ev 2018, Faulkner et al., 2019).

Atomic units will be used throughout unless otherwise stated.

2. THEORY

We consider single-electron capture in collisions between fast completely stripped projectiles and hydrogen-like ion targets, according to the following relations:

$$Z_P + (Z_T, e)_{1s} \rightarrow (Z_P, e)_{nlm} + Z_T, \tag{1}$$

$$Z_P + (Z_T, e)_{1s} \rightarrow (Z_P, e)_{nl} + Z_T, \tag{2}$$

$$Z_P + (Z_T, e)_{1s} \rightarrow (Z_P, e)_n + Z_T, \quad (3)$$

$$Z_P + (Z_T, e)_{1s} \rightarrow (Z_P, e)_\Sigma + Z_T, \quad (4)$$

where Z_P and Z_T are the charges of the projectile P and target nucleus T, respectively, while e denotes the electron. Relation (1) represents single-electron capture which occurs from the ground state $1s$ of the hydrogen-like target, into an arbitrary nlm final state of the projectile, where $\{n, l, m\}$ is the usual triplet of quantum numbers. Relations (2) and (3) represent capture from the ground state into arbitrary subshells nl and shells n, respectively, while relation (4) denotes single-electron capture from the ground into all final states of the projectile.

The transition amplitude matrix elements T_{if} in the prior form of the CB1-3B method for process (1) are given by the following equation:

$$T_{if}^{CB1}(\vec{\eta}) = Z_P \int\int d\vec{s} d\vec{R}\, \varphi_{nlm}^*(\vec{s}) \left(\frac{1}{R} - \frac{1}{s}\right) \varphi_{100}(\vec{x}) e^{i\vec{\beta}\cdot\vec{R} - i\vec{v}\cdot\vec{s}} \left(vR + \vec{v}\cdot\vec{R}\right)^{i(\xi - \nu_T)}, \quad (5)$$

whereas in the prior form of the BCIS-3B method they are given by (Milojević et al., 2020):

$$T_{if}^{BCIS}(\vec{\eta}) = N^+(\nu_T) Z_P \int\int d\vec{s} d\vec{R}\, \varphi_{nlm}^*(\vec{s}) \left(\frac{1}{R} - \frac{1}{s}\right) \varphi_{100}(\vec{x}) e^{i\vec{\beta}\cdot\vec{R} - i\vec{v}\cdot\vec{s}}$$

$$\times F(i\nu_T, 1, ivx + i\vec{v}\cdot\vec{x}) \left(vR + \vec{v}\cdot\vec{R}\right)^{i\xi}, \quad (6)$$

where we introduced the symbols $\xi = Z_P/v$, $\nu_T = Z_T/v$ and $N^+(\nu_T) = \Gamma(1 - i\nu_T) e^{\pi\nu_T/2}$. Here $\vec{v}$ is the projectile velocity along the z-axis, while $\vec{\beta} = -\vec{\eta} - \beta_z \hat{\vec{v}}$ is the momentum transfer, with its component along the $z-$axis being $\beta_z = v/2 + \Delta E/v$. Further, $\Delta E = E_i - E_f$ is the difference between the initial and final bound state energies, while $\vec{\eta} = \left(\eta\, cos\, \phi_\eta\, , \eta\, sin\, \phi_\eta\, , 0\right)$ is the transverse momentum transfer vector, with the property $\vec{\eta}\cdot\vec{v} = 0$. The position vectors of the electron relative to the target and projectile are denoted by $\vec{x}$ and $\vec{s}$, respectively, while the relative position vector of the projectile to the target is denoted by $\vec{R}$. The hydrogen-like wavefunction $\varphi_{100}(\vec{x})$ is the ground state wavefunction of the target ion $(Z_T, e)_{1s}$, while $\varphi_{nlm}(\vec{s})$ is the arbitrary state wavefunction of the projectile system $(Z_P, e)_{nlm}$ formed after the collision. Finally, the confluent hypergeometric function is denoted by $F(i\nu_T, 1, ivx + i\vec{v}\cdot\vec{x})$.

The original integrals for the transition amplitude matrix elements $T_{if}^{CB1/BCIS}$ appearing in Equations (5) and (6) are six-dimensional. However, through suitable mathematical manipulations, some of these integrals can be analytically solved, so that T_{if}^{CB1} can be reduced to a one-dimensional, while T_{if}^{BCIS} can be reduced to a two-dimensional integral over real variables in the interval $[0,1]$. The state-selective total cross sections $Q_{nlm}^{CB1/BCIS}$ for capture into an arbitrary final state nlm of the projectile are then given by:

$$Q_{nlm}^{CB1/BCIS}(a_0^2) = \frac{1}{2\pi v^2} \int_0^\infty d\eta\eta \left|T_{if}^{CB1/BCIS}(\vec{\eta})\right|^2, \quad (7)$$

and are two-dimensional integrals over real variables in the CB1-3B case, while in the BCIS-3B approach they are three-dimensional (also over real variables). The state-selective total cross sections for capture into nl subshells and n shells are then, respectively, given by:

$$Q_{nl}^{CB1/BCIS} = \sum_{m=-l}^{+l} Q_{nlm}^{CB1/BCIS}, \quad Q_{n}^{CB1/BCIS} = \sum_{l=0}^{n-1} Q_{nl}^{CB1/BCIS}. \tag{8}$$

For the purposes of this paper, state-selective total cross sections were calculated up to $n = 4$. The contributions to the state-summed total cross sections from higher excited final states were included via the Oppenheimer n^{-3} scaling law (Oppenheimer, 1928):

$$Q^{CB1/BCIS} \equiv Q_{\Sigma}^{CB1/BCIS} = Q_{1}^{CB1/BCIS} + Q_{2}^{CB1/BCIS} + Q_{3}^{CB1/BCIS} + 2.561 Q_{4}^{CB1/BCIS}. \tag{9}$$

For performing numerical integrations in Equation (7), Gauss-Legendre quadrature rules were employed. In the CB1-3B method, only 96 integration points per each of the two integration axes were sufficient to achieve a convergence of at least two decimal places for both the state-selective and state-summed total cross sections, in the whole energy interval considered. In the BCIS-3B method, at both lower and higher ends of the considered energy interval, a total of 1616 integration points were needed along each of the three integration axes, in order for the state-selective and state-summed total cross sections to converge at the level of 1%. More problematic in this regard was the lower end interval of incident projectile energy. Moreover, it has been determined that at higher energy values higher projectile charges correspond to a better convergence for numerical integrations. The convergence at lower energy values does not substantially depend upon the projectile charge. Higher target charges, while also improving convergence at higher energy values, simultaneously slow the convergence of integrals at lower incident energy values. Also, at higher energy values and for a given collisional system, integrals converge more slowly for higher n shells. All these considerations allow for a more systematic approach to dealing with convergence issues, which inevitably arise in the BCIS-3B case. Another noteworthy point for the BCIS-3B approach is that Cauchy regularization was employed before performing numerical integration.

3. Results and Discussion

In this work, we consider the following processes with single-electron capture:

$$p + \mathrm{He}^{+}(1s) \rightarrow \mathrm{H}(\Sigma) + \alpha, \tag{10}$$

$$\alpha + \mathrm{He}^{+}(1s) \rightarrow \mathrm{He}^{+}(\Sigma) + \alpha, \tag{11}$$

$$\alpha + \mathrm{Li}^{2+}(1s) \rightarrow \mathrm{He}^{+}(\Sigma) + \mathrm{Li}^{3+}, \tag{12}$$

$$\mathrm{Li}^{3+} + \mathrm{Li}^{2+}(1s) \rightarrow \mathrm{Li}^{2+}(\Sigma) + \mathrm{Li}^{3+}, \tag{13}$$

where p and α represent a proton (hydrogen ion H^{+}) and an alpha particle (completely stripped helium He^{2+}), respectively. For all the listed processes (10)-(13), we calculated the state-summed total cross section in both the CB1-3B and BCIS-3B methods, and graphically represented the results in Figures 1-4. Whenever possible, comparisons of the present theoretical results with the available experimental data were made. What needs to be stressed, however, is that all the measurements were made for intermediate energy values, with no experimental results being available for incident energy higher than 175 keV. This presents a setback for benchmarking the CB1-3B and BCIS-3B theories for processes (10)-(13), since there are no high energy measurements performed, for which the presented methods are expected to produce the best results. Nevertheless, these

methods are known to be in excellent agreement with experiments even for intermediate energy values, and in certain cases at energies as low as 8 keV (Milojević et al., 2020). Therefore, the available measurements should still be relevant from the present theoretical standpoint.

Figure 1 shows the present theoretical results for process (10), along with a comparison with the available experimental data from three different sets of measurements Peart et al., 1983, Rinn et al., 1985, and Watts et al., 1986. Note that all three sets of measurements are in good mutual accord. As can be seen from Figure 1, CB1-3B results excellently reproduce the measurements for $E \geq 40$ keV, up to the highest energy measurement available, at $E = 175$ keV. The BCIS-3B results underestimate the measurements in available energy interval, but with the agreement improving for increasing energy, and becoming satisfactory for $E \geq 80$ keV. The BCIS-3B results slightly overestimate the CB1-3B results in the $80\ \text{keV} \leq E \leq 220$ keV region, while they underestimate them in the rest of the displayed energy intervals.

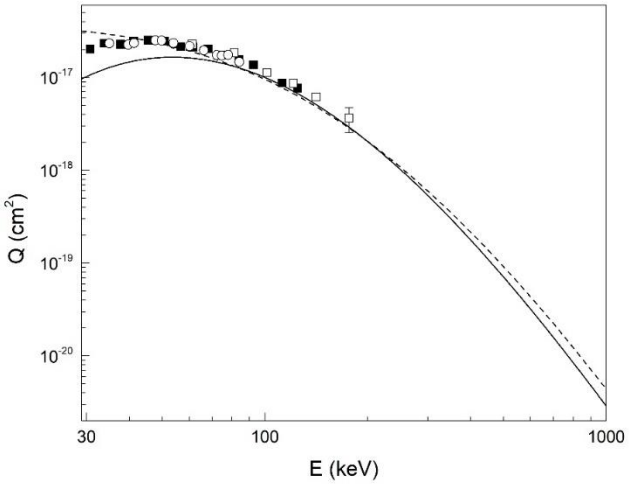

Fig. 1 State-summed total cross sections $\boldsymbol{Q_\Sigma \equiv Q}(\text{cm}^2)$ for process $\boldsymbol{p + He^+(1s) \rightarrow H(\Sigma) + \alpha}$ as a function of laboratory incident energy $\boldsymbol{E}$ (keV). The present theoretical results are represented by the full line for the BCIS-3B method, and by the dashed line for the CB1-3B method. Experimental data: ○ Peart et al., 1983, ■ Rinn et al., 1985, □ Watts et al., 1986.

Figure 2 shows the present results for process (11), with a single available set of experimental data Melchert et al., 1995 also being displayed. The situation here as in the case of process (10), i.e. CB1-3B being in better agreement with the experiment. The agreement between the theories and the experiment is, although very good, a bit worse in this case than in the previous one. The CB1-3B results are in very good agreement with the measurement for $E \geq 50$ keV/amu, while BCIS-3B results approach the experiment for $E \geq 90$ keV/amu. Both lower limits have slightly higher values than in process (10). Nevertheless, the theories still provide a very satisfactory reproduction of the experimental

results for process (11), despite the highest energy measurement made for only $115\,\mathrm{keV/amu}$, which is an intermediate energy value. One can also note that BCIS-3B results overestimate CB1-3B ones in the energy range $30\,\mathrm{keV/amu} \leq E \leq 500\,\mathrm{keV/amu}$, while this trend inverts for higher energy values.

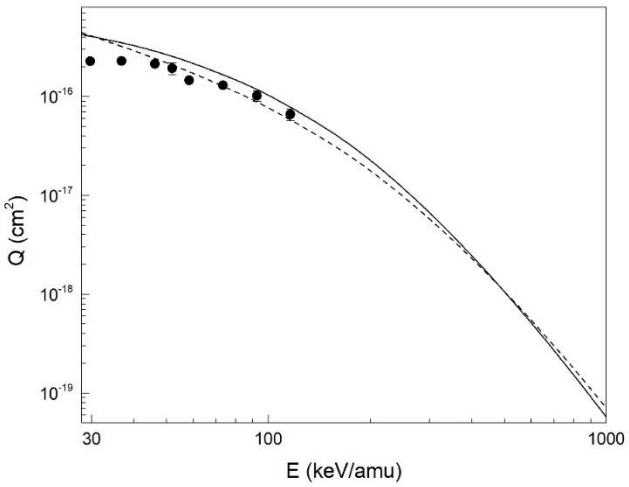

Fig. 2 State-summed total cross sections $\boldsymbol{Q_\Sigma \equiv Q}(\mathrm{cm}^2)$ for process $\boldsymbol{\alpha + He^+(1s) \rightarrow He^+(\Sigma) + \alpha}$ as a function of laboratory incident energy $\boldsymbol{E}$ $(\mathrm{keV/amu})$. The present theoretical results are represented by the full line for the BCIS-3B method, and by the dashed line for the CB1-3B method. Experimental data: ● Melchert et al., 1995.

The present theoretical results for process (12), along with a comparison with the experimental data set of Brauning et al., 2005, is depicted in Figure 3. The experimental results are from the energy interval $30\,\mathrm{keV/amu} \leq E \leq 70\,\mathrm{keV/amu}$, which is even further away from the high energy region. Neither of the two applied methods successfully reproduces the experimental results, with the CB1-3B method significantly overestimating them, while BCIS-3B fares slightly better, although still underestimates the measurements in the whole energy range. Take note that BCIS-3B, however, does approach the experimental results within the measurement error, at least for certain experimental points. Further, below $165\,\mathrm{keV/amu}$, CB1-3B results overestimate BCIS-3B ones, while for $E \geq 165\,\mathrm{keV/amu}$ both produce more or less the same results (with BCIS-3B results very slightly overestimating CB1-3B results for $165\,\mathrm{keV/amu} \leq E \leq 630\,\mathrm{keV/amu}$, and slightly underestimating it for $630\,\mathrm{keV/amu} \leq E \leq 1000\,\mathrm{keV/amu}$). The theories seem to largely diverge for the lowest energy values.

Finally, Figure 4 gives the present theoretical results for process (13). There are no measurements available to make a comparison with. Still, one can see that CB1-3B results overestimate BCIS-3B results for $E \leq 70\,\mathrm{keV/amu}$, while the situation is opposite for $70\,\mathrm{keV/amu} \leq E \leq 1000\,\mathrm{keV/amu}$. The BCIS-3B theoretical results again display a larger curvature than the CB1-3B ones. Until some measurements in at least

intermediate and preferably high energy regions are made, nothing more can, unfortunately, be said regarding the validity of the present results for process (13).

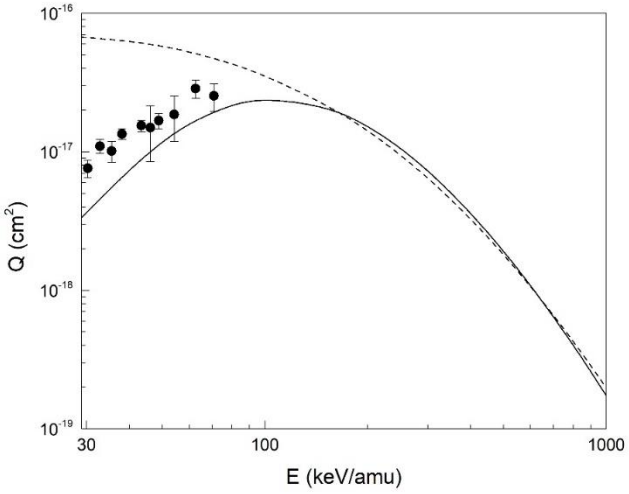

Fig. 3 The same as in Fig. 2, but for process $\boldsymbol{\alpha} + \mathrm{Li}^{2+}(1s) \rightarrow \mathrm{He}^{+}(\Sigma) + \mathrm{Li}^{3+}$. Experimental data: ● Brauning et al., 2005.

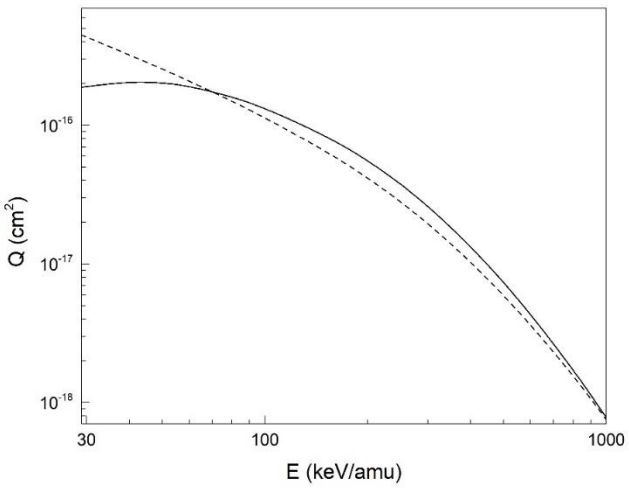

Fig. 4 The same as in Fig. 2, but for process $\mathrm{Li}^{3+} + \mathrm{Li}^{2+}(\mathbf{1s}) \rightarrow \mathrm{Li}^{2+}(\Sigma) + \mathrm{Li}^{3+}$.

To sum up the observations from all processes discussed (10)-(13), we can conclude that CB1-3B and BCIS-3B methods produce very similar state-summed total cross sections for higher energy values, while the difference between them generally becomes more pronounced as we approach the lower limits of energy values displayed. In comparison with the experimental results, we see that both methods produce a satisfactory agreement for processes (10) and (11), with CB1-3B better reproducing the measurements. For process (12), however, neither methods are sufficiently good, with BCIS-3B being more adequate. In addition, all measurements for these three processes (10)-(12) were made for intermediate energy values, with no available experimental data for higher energies. Therefore, these energies are outside the primary scope of application of high energy methods, such as CB1-3B and BCIS-3B. Nevertheless, in all considered cases, both methods become more and more adequate as the incident energy rises. Therefore, possible future measurements at higher energy values are expected to even further affirm the CB1-3B and BCIS-3B methods. Another important observation is that the lower energy limit of the validity of the two theories seems to increase with rising charges of the projectile Z_P and target nucleus Z_T. The reason for this would be the rising magnitude of the Coulomb interaction, which increases the lower limits of applicability of high energy theories. Finally, for process (13), there are unfortunately no available measurements to make a comparison with.

4. CONCLUSION

This paper was dedicated to the single-electron capture process in collisions between hydrogen-like ions and fully-stripped projectiles. Concretely, state-summed total cross sections were calculated for single-electron capture in $p + \mathrm{He}^+$, $\alpha + \mathrm{He}^+$, $\alpha + \mathrm{Li}^{2+}$ and $\mathrm{Li}^{3+} + \mathrm{Li}^{2+}$ collisions, where the target ions were in the ground states. Explicit contributions up to $n = 4$ were considered, with the contributions from higher shells included via the Oppenheimer scaling law. The calculations were carried out in the frameworks of the CB1-3B and BCIS-3B methods. Overall, a satisfactory agreement between both theoretical methods and the available experimental results were obtained for $p + \mathrm{He}^+$ and $\alpha + \mathrm{He}^+$ collisions, with CB1-3B being more adequate. The BCIS-3B method produces better results for process $\alpha + \mathrm{Li}^{2+}$, although none of these methods agree particularly well with the available measurements. Unfortunately, no experimental data is available for process (13). Since all measurements were performed at intermediate energy values, an even better agreement is expected at high energies, where the domain of applicability of the presented theories truly lies. Possible future measurements performed at higher energy values would be highly anticipated here, since they are expected to confirm the previous statement, particularly since the agreement between the theories and measurements manifestly improves with increasing energy. Nevertheless, even in comparison with the intermediate energy measurements already available, the validity of the CB1-3B and BCIS-3B methods is indeed even further confirmed by this work.

REFERENCES

Belkić, Dž., Gayet, R., Salin, A., 1979. Phys. Rep., 56, 279–369. doi:10.1016/0370-1573(79)90035-8
Belkić, Dž., Gayet, R., Hanssen, J., Salin, A., 1986. J. Phys. B: At. Mol. Phys., 19, 2945–2953. doi:10.1088/0022-3700/19/18/023
Belkić, Dž., Taylor, H. S., 1987. Phys. Rev. A, 35, 1991–2006. doi:10.1103/PhysRevA.35.1991
Belkić, Dž., Saini, S., Taylor, H. S., 1987b. Phys. Rev. A, 36, 1601–1617. doi:10.1103/PhysRevA.36.1601
Belkić, Dž., 1993. Phys. Rev. A, 47, 3824–3844. doi:10.1103/PhysRevA.47.3824
Belkić Dž., 2004. Principles of Quantum Scattering Theory, Institute of Physics, Bristol
Belkić, Dž., 2008. Quantum Theory of High-Energy Ion-Atom Collisions, Taylor & Francis, London
Brinkman, H. C., Kramers, H. A., 1930. Proc. Acad. Sci. Amsterdam, 33, 973–984.
Brauning, H., Trassl, R., Theiß, A., Diehl, A., Salzborn, E., Keim, M., Achenbach, A., Ludde, H. J., Kirchner, T., 2005. J. Phys. B: At. Mol. Opt. Phys., 38, 2311–2317. doi:10.1088/0953-4075/38/13/022
Faulkner, J., Abdurakhmanov, I. B., Alladustov, Sh. U., Kadyrov, A. S., Bray, I., 2019. Plasma Phys. Control. Fusion, 61, 095005. doi:10.1088/1361-6587/ab2e7a
Grozdanov, T., Solov'ev, E., 2018. Eur. Phys. J. D, 72, 64. doi:10.1140/epjd/e2018-80758-x
Mančev, I., Milojević, N., Belkić, Dž., 2012. Phys. Rev. A, 86, 022704. doi: 10.1103/PhysRevA.86.022704
Mančev, I., Milojević, N., Belkić, Dž., 2015. Phys. Rev. A, 91, 062705. doi: 10.1103/PhysRevA.91.062705
Mančev, I., Milojević, N., Belkić, Dž., 2018. Eur. Phys. J. D, 72, 209. doi:10.1140/epjd/e2018-90290-8
Milojević, N., Mančev I., Delibašić D., Belkić Dž., 2020. Phys. Rev. A, 102, 012816. doi: 10.1103/PhysRevA.102.012816
Mukherjee, S., Sil, N. C., 1980. J. Phys. B: At. Mol. Phys., 13, 3421–3430. doi:10.1088/0022-3700/13/17/020
Melchert, F., Krudener, S., Schulze, R., Petri, S., Pfaff, S., Salzborn, E., 1995. J. Phys. B: At. Mol. Opt. Phys., 28, L355–L359. doi:10.1088/0953-4075/28/10/005
Oppenheimer, J. R., 1928. Phys. Rev., 31, 349–356. doi:10.1103/PhysRev.31.349
Peart, B., Rinn, K., Dolder, K., 1983. J. Phys. B: At. Mol. Phys., 16, 1461–1469. doi: 10.1088/0022-3700/16/8/019
Rinn, K., Melchert, F., Salzborn, E., 1985. J. Phys. B: At. Mol. Phys., 18, 3783–3795. doi: 10.1088/0022-3700/18/18/019
Samanta, R., Purkait, M., Mandal C. R., 2010. Phys. Scr., 82, 065303. doi:10.1088/0031-8949/82/06/065303
Watts, M. F., Dunn K. F., Gilbody H. B., 1986. J. Phys. B: At. Mol. Opt. Phys., 19, L355–L359. doi:10.1088/0022-3700/19/10/005

JEDNOSTRUKI ELEKTRONSKI ZAHVAT U JON-JONSKIM SUDARIMA

Prethodne verzije tročestične granično korektne prve Bornove aproksimacije (CB1-3B) i tročestičnog granično korektnog metoda sa kontinuumskim intermedijarnim stanjima (BCIS-3B) su primenjene na izračunavanje parcijalnih i sumiranih totalnih preseka za jednostruki elektronski zahvat iz vodoniku sličnih jonskih meta (He^+, Li^{2+}) *pri sudaru sa brzim potpuno ogoljenim projektilima* (H^+, He^{2+}, Li^{3+}). *Sva izračunavanja su urađena za jednostruki elektronski zahvat u proizvoljna nlm finalna stanja projektila, do* $n = 4$. *Doprinosi od ljuski sa većim vrednostima* n *su uračunati korišćenjem Openhajmerovog* n^{-3} *zakona skaliranja. Dobijeni rezultati su u zadovoljavajućoj saglasnosti sa dostupnim eksperimentalnim podacima.*

Ključne reči: *jon-jonski sudari, elektronski zahvat*